AMERICAN SOCIETY FOR MICROBIOLOGY | Microbiology Spectrum

RESEARCH ARTICLE

High Growth Rate of Diatoms Explained by Reduced Carbon Requirement and Low Energy Cost of Silica Deposition

Keisuke Inomura,[a] Juan José Pierella Karlusich,[b,c] Stephanie Dutkiewicz,[d] Curtis Deutsch,[e] Paul J. Harrison,[f] Chris Bowler[b]

[a]Graduate School of Oceanography, University of Rhode Island, Narragansett, Rhode Island, USA
[b]Institut de Biologie de l'Ecole Normale Supérieure, CNRS, INSERM, Université Paris Sciences et Lettres, Paris, France
[c]Faculty of Arts and Sciences, Division of Science, Harvard University, Cambridge, Massachusetts, USA
[d]Department of Earth, Atmospheric, and Planetary Sciences, Massachusetts Institute of Technology, Cambridge, Massachusetts, USA
[e]Department of Geosciences, Princeton University, Princeton, New Jersey, USA
[f]Department of Earth, Ocean, and Atmospheric Sciences, University of British Columbia, Vancouver, British Columbia, Canada

ABSTRACT The rapid growth of diatoms makes them one of the most pervasive and productive types of plankton in the world's ocean, but the physiological basis for their high growth rates remains poorly understood. Here, we evaluate the factors that elevate diatom growth rates, relative to other plankton, using a steady-state metabolic flux model that computes the photosynthetic C source from intracellular light attenuation and the carbon cost of growth from empirical cell C quotas, across a wide range of cell sizes. For both diatoms and other phytoplankton, growth rates decline with increased cell volume, consistent with observations, because the C cost of division increases with size faster than photosynthesis. However, the model predicts overall higher growth rates for diatoms due to reduced C requirements and the low energetic cost of Si deposition. The C savings from the silica frustule are supported by metatranscriptomic data from *Tara* Oceans, which show that the abundance of transcripts for cytoskeleton components in diatoms is lower than in other phytoplankton. Our results highlight the importance of understanding the origins of phylogenetic differences in cellular C quotas, and suggest that the evolution of silica frustules may play a critical role in the global dominance of marine diatoms.

IMPORTANCE This study addresses a longstanding issue regarding diatoms, namely, their fast growth. Diatoms, which broadly are phytoplankton with silica frustules, are the world's most productive microorganisms and dominate in polar and upwelling regions. Their dominance is largely supported by their high growth rate, but the physiological reasoning behind that characteristic has been obscure. In this study, we combine a quantitative model and metatranscriptomic approaches and show that diatoms' low carbon requirements and low energy costs for silica frustule production are the key factors supporting their fast growth. Our study suggests that the effective use of energy-efficient silica as a cellular structure, instead of carbon, enables diatoms to be the most productive organisms in the global ocean.

KEYWORDS *Tara* Oceans, computer modeling, diatom, ecosystem, growth, microbiology, oceanography, photosynthesis, phytoplankton, silica frustule

Diatoms are major photosynthesizers in the ocean, accounting for up to 45% of marine primary production, more than that of all the world's tropical rainforests (1). Diatoms are uniquely characterized by silica (SiO_2) frustules (shell) (2–7) and display a diverse set of molecular responses to environmental conditions (8–10). They are major components of the ecosystem at high latitudes and in coastal regions where nutrients are abundant (11–13). Such dominance requires high growth rates, which enable populations to proliferate rapidly under conditions with high nutrient levels (14–16). The global niches of diatoms

Editor Allison Veach, University of Texas at San Antonio

Copyright © 2023 Inomura et al. This is an open-access article distributed under the terms of the Creative Commons Attribution 4.0 International license.

Address correspondence to Keisuke Inomura, inomura@uri.edu.

This article is contribution number 143 from *Tara* Oceans.

The manuscript is dedicated to the memory of Paul J. Harrison.

The authors declare no conflict of interest.

[This article was published on 3 April 2023 with errors in the supplemental material. The supplemental material was corrected on 6 April and in the current version, posted on 25 April 2023.]

Received 20 August 2022
Accepted 2 March 2023
Published 3 April 2023

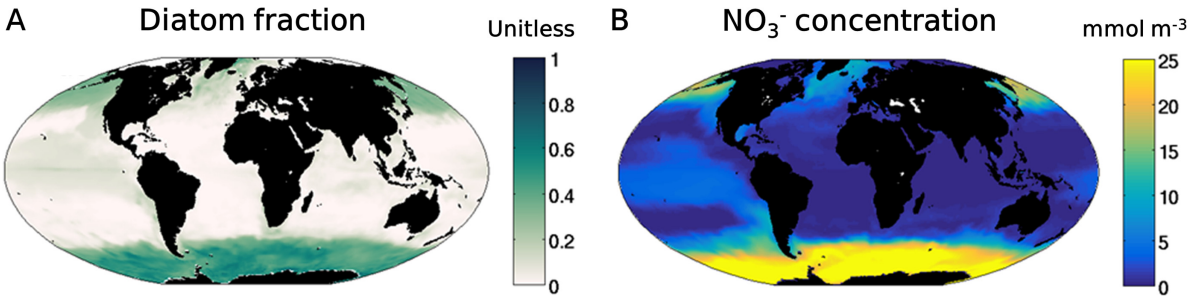

FIG 1 Recent simulations of the fraction of global diatom biomass and nitrate concentrations. The fraction of diatom biomass (A) and NO_3^- concentrations (B) were simulated with the marine ecological model MITgcm (19). These plots show that the annual means averaged between 0 m and 50 m in depth. The general distribution patterns are consistent with observations (see Fig. S6 in reference 19).

can be captured in marine ecosystem models with the assumption that they have the highest maximum growth rate among the phytoplankton, with a trade-off of a high half-saturation constant (17–20) (output from the model in reference 19 is shown in Fig. 1). The high growth rate in combination with lower palatability allows diatom dominance in environments with high/fluctuating levels of nutrients, whereas other plankton may have advantages in environments with stable low levels of nutrients, where high nutrient affinities are favored (19).

High maximum growth rates for diatoms assumed by ecosystem models are largely consistent with laboratory observations of growth rates under nutrient-replete conditions, despite considerable variations (21–23) (Fig. 2, circles). However, the causes of such high diatom growth rates remain elusive. It has been suggested that the production of the silica frustule is energetically efficient (24, 25), yet such an effect has not been quantitatively analyzed at a cellular scale. How does energy efficiency influence the growth of diatoms? Diatoms have also been found to have a low C (carbon) per volume, relative to other phytoplankton, e.g., a compilation of cellular C-volume relationships shows that diatoms display a lower C per specific volume than other phytoplankton (26), suggesting that the C cost of reproduction for a given cell size should be lower for diatoms. How does this pattern influence the growth rate?

In addition to the high growth rate of diatoms, there is a clear trend between cell volumes and growth rates. Above the cell volume of 10^2 μm^3, the growth rates of diatoms and other phytoplankton decrease (Fig. 2) (23, 27–30). Multiple theories have been proposed for this trend. First, increasing cell size increases intracellular distances (for example, between organelles), thus decreasing the speed of molecular transport and processing and decreasing the growth rate (30, 31). Second, increasing cell size increases the packaging effect (intracellular light absorption), thus decreasing the photosynthesis rate per volume and decreasing the growth rate (30, 32). To test this effect in the context of whole-cell metabolism, here we develop a model (Cell Flux model of a Diatom [CFM-Diatom]) (Fig. 3) by combining a

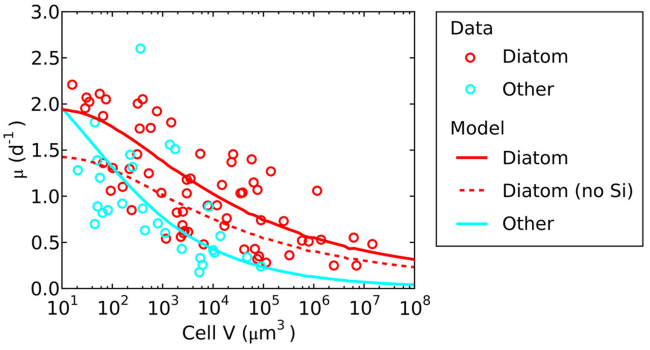

FIG 2 Model data comparison of nutrient-replete growth rate (μ)-cell volume (V) relationships. Data are from reference 23. Other includes chlorophytes, dinoflagellates, coccolithophores, haptophytes, and raphidophytes. Diatom (no Si) indicates the simulation with the C cost of non-silica biomass production applied to silica frustule production.

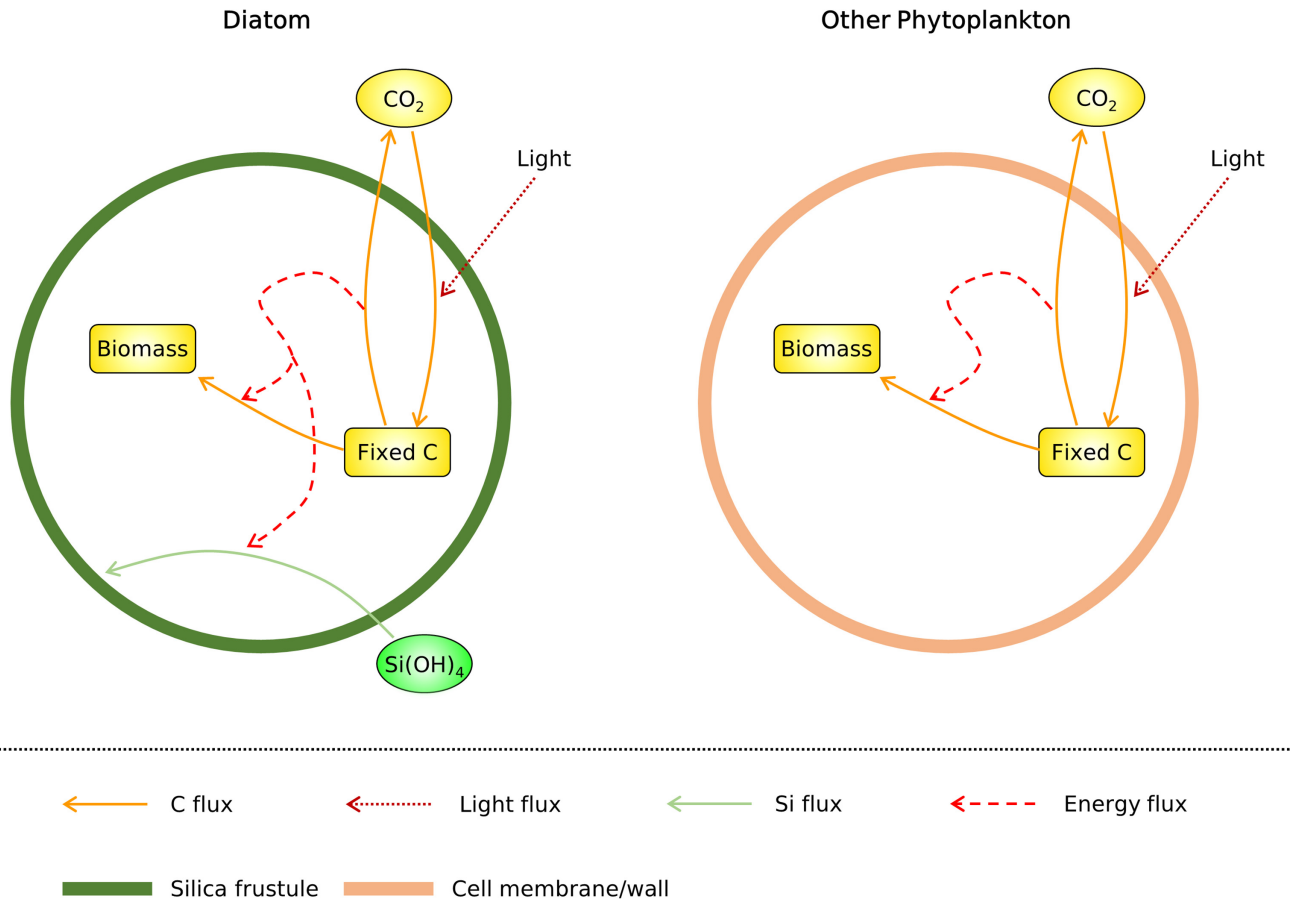

FIG 3 Schematics of the coarse-grained models of diatoms (CFM-Diatom) and non-diatom phytoplankton. Here, biomass represents all of the final cellular material that contains carbon.

simple model of light absorption within a cell with a cellular model of simple metabolism (33–35) to analyze the general trends in nutrient-replete growth rates across orders of magnitude of cell size.

RESULTS AND DISCUSSION

Model prediction of the growth rates. CFM-Diatom is a simple metabolic flux model that resolves essential metabolism, including C fixation (photosynthesis), respiration, generation of biomass, and silica deposition (Fig. 3). These fluxes are constrained by mass, electron, and energy balances under a steady-state assumption. The model also resolves the effect of intracellular light attenuation. The model differentiates diatoms from other phytoplankton on the basis of the existence of silica deposition and cellular C per volume (details in Materials and Methods). Despite its simplicity, the model captures the general trend of growth rate-cell volume relationships for both diatoms and other phytoplankton (Fig. 2). The growth rates of diatoms and other phytoplankton decrease with increased cell volume, but diatoms have higher growth rates at a specific volume, consistent with the compiled data (Fig. 2).

Intracellular light attenuation results in lower growth rates with larger cell volumes. The general trend of decreasing growth rate with increasing cell volume is predicted as a consequence of intracellular light attenuation (Fig. 2 and 4). As the cell volume increases, the path length of light increases within the cell, reducing light intensity per volume of the cell. This effect leads to a lower per-volume rate of photosynthesis (Fig. 4A) and a decreased slope of the cellular photosynthesis rate-volume relationship (Fig. 4B). This decreased slope, in turn, results in decreased growth rates with increased cell volume (Fig. 2), since the

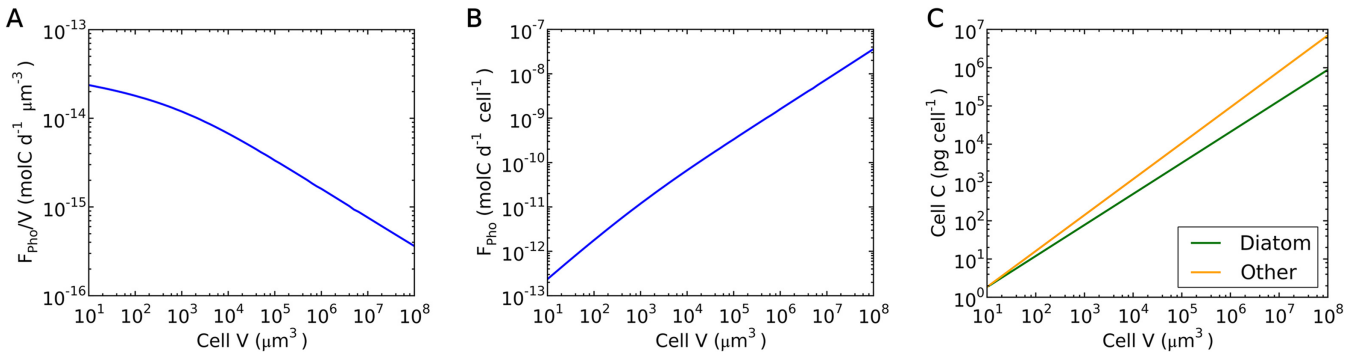

FIG 4 Simulated photosynthesis rates for different cell volumes and observed relationships between cellular C and cell volume. (A) Simulated photosynthesis rate (per volume)-volume relationship. (B) Simulated photosynthesis rate (per cell)-volume relationship. (C) Cellular C-volume relationship of diatoms and other phytoplankton (26).

cellular C does not decrease as severely with increased volume (Fig. 4C), and the growth rate is proportional to the photosynthesis rate per cellular C (F_{Pho}/Q_C).

Low C requirement and low energetic cost of silica deposition support high growth rates of diatoms. What explains the differences in growth rate between diatoms and other phytoplankton? Our model predicts the observed difference (Fig. 2), based on the reduced C requirement per cell (Fig. 4C) and the extremely low cost of silica deposition (Fig. 5). The reduced C requirement is based on the compilation of Q_C versus size for different taxa of phytoplankton (26). It has been shown that diatoms follow a distinct curve, compared with other taxa, with lower Q_C values (Fig. 4C). We applied this relationship in the model with the observed different values for A_C and B_C (26) and reproduced the observed trend by using the same rate of photosynthesis for diatoms and non-diatoms. The predicted growth rate of diatoms due to the higher specific rates of photosynthesis (photosynthesis rate per C) are because of the lower cellular C; this is qualitatively supported by the observation of a relatively high content of chlorophyll per C in diatoms (36). Other physiological factors could potentially contribute to high specific photosynthesis rates of diatoms, such as carbon concentration mechanisms (37–39), chloroplast-mitochondrion coupling (40), and the use of silica frustules for enhanced light harvesting (41).

Although the C requirement for diatoms is small, there is a cost specific to diatoms, i.e., silica deposition. Although the cost for silica deposition per Si (silicon) has been

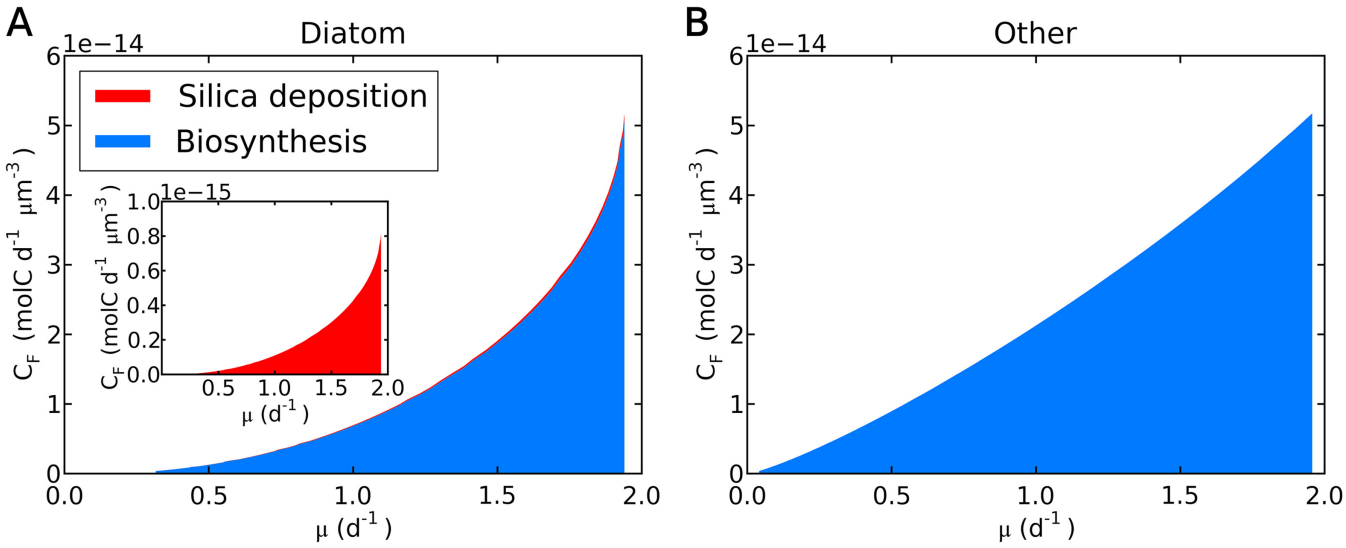

FIG 5 Simulated fate of C (C_F) for various growth rates under nutrient repletion. (A) Diatoms. (B) Other phytoplankton of the same size. The *y* axes indicate C flux per cell volume. In panel A, there is a slight layer in red (C cost for silica deposition) on top of the blue (C cost for biosynthesis); the C for silica deposition is almost invisibly small. To make it visible, the inset shows C cost for silica deposition with a different range on the *y* axis.

estimated (24, 25), the silica deposition cost relative to the entire C cost has not been quantified. Our model shows that the C cost for silica deposition is minimal, accounting for only ~1.6% of the entire carbon cost (Fig. 5A), which includes C for biosynthesis and C for respiration to support biosynthesis. This prediction of a low cost of Si is partially due to the low C cost per Si (0.167 mol C mol Si^{-1}), compared to the C costs per biomass C production ($1 + E_\mu$) (1.691 mol C mol C^{-1}), and partially due to the relative amounts of Si versus C (here, 0.163 [maximum value from reference 42]) (see Table S2 in the supplemental material). Despite the application of a Si/C ratio at the high end of the observed range (42), the total energy cost of silica deposition is small, suggesting that the energetic effect of variations in Si/C is negligible on a cellular scale. Although the cells could have even higher Si content, especially with excess Si availability (43, 44), the results of total C cost and growth rate would not change significantly (e.g., see Fig. S2) since the silica deposition cost is extremely small. On the other hand, if we apply the C cost of non-silica biomass production to the production of silica frustule, the model predicts substantially lowered growth rate (Fig. 2; compare dashed and solid red curves), underpinning the importance of low Si cost.

Hypothesis arising from this study: Si replacement of C in structural material. The model results show that the reduced C requirement and low energetic costs could be key factors underlying the high growth rate of diatoms. This leads us to hypothesize that, quantitatively, Si takes over some functional roles of C, reducing C demand and energetic costs and leading to a high growth rate. For example, cells need proteins to maintain their structure (e.g., cytoskeleton) (45, 46). Also, phytoplankton typically have cell walls that support cell morphology (47–49). These C-rich structural molecules may be reduced in diatoms, since their silica frustules provide the rigid support for maintaining cell structure. While diatoms may require additional resources to construct their silica frustules, we predict that the resource requirement is minimal because the template contains only one layer of amino acid residues (2).

Although silica frustules may provide structural support, the frustules cannot replace molecules that are related to growth, since they do not generally facilitate biochemical processes as enzymes do. For example, they cannot replace photosystems and enzymes for C fixation. As a result, the C-specific abundance of these synthesis-facilitating molecules increases as the C-rich structure is replaced by the silica frustules. We point out that vacuoles may be one of the causes of low C content (26), which would reduce the intracellular space for photosynthetic molecules. Also, it is possible that vacuoles are rather the outcome of reduced structural material.

Exploring the hypothesis with *Tara* Oceans data: diatoms invest high transcriptional efforts into protein synthesis but not into cytoskeleton maintenance. At steady state, the growth rate of phytoplankton depends on the protein synthesis capacity of the cell and thus on the number of active ribosomes (50, 51). Here, we examined the metatranscriptomes from samples collected by *Tara* Oceans from the main ocean basins (52, 53) (Fig. 6) to determine the proportion of transcripts coding for ribosomal proteins among the different phytoplankton taxa. Our results showed that diatoms generally have greater relative abundances of transcripts for ribosomal proteins than do the other phytoplankton groups (Fig. 6), possibly reflecting their higher growth rates due to the replacement of some cellular C by Si.

In addition, the rigid support of the silica frustule can reduce diatom efforts in maintaining their structure using the cytoskeleton. We examined this possibility by analyzing the relative abundances of transcripts coding for the main cytoskeleton components, actin and tubulin, and found that diatoms indeed have lower levels of transcripts for them, in comparison with other phytoplankton groups (Fig. 6).

Our model focuses on the general trend of the growth rates for diatoms versus nondiatoms. Thus, it mainly focuses on the averaged pattern. However, there are significant variations even within a diatom group. Morphologically, some are chain-forming and others are solitary. Some are found in freshwater, while others are found in marine environments. Even within the ocean, some exist in coastal environments, while others are found in the open ocean. Furthermore, different diatoms contribute differently to the biological carbon pump (54). Possibly due to these differences, our data show considerable variations. Despite

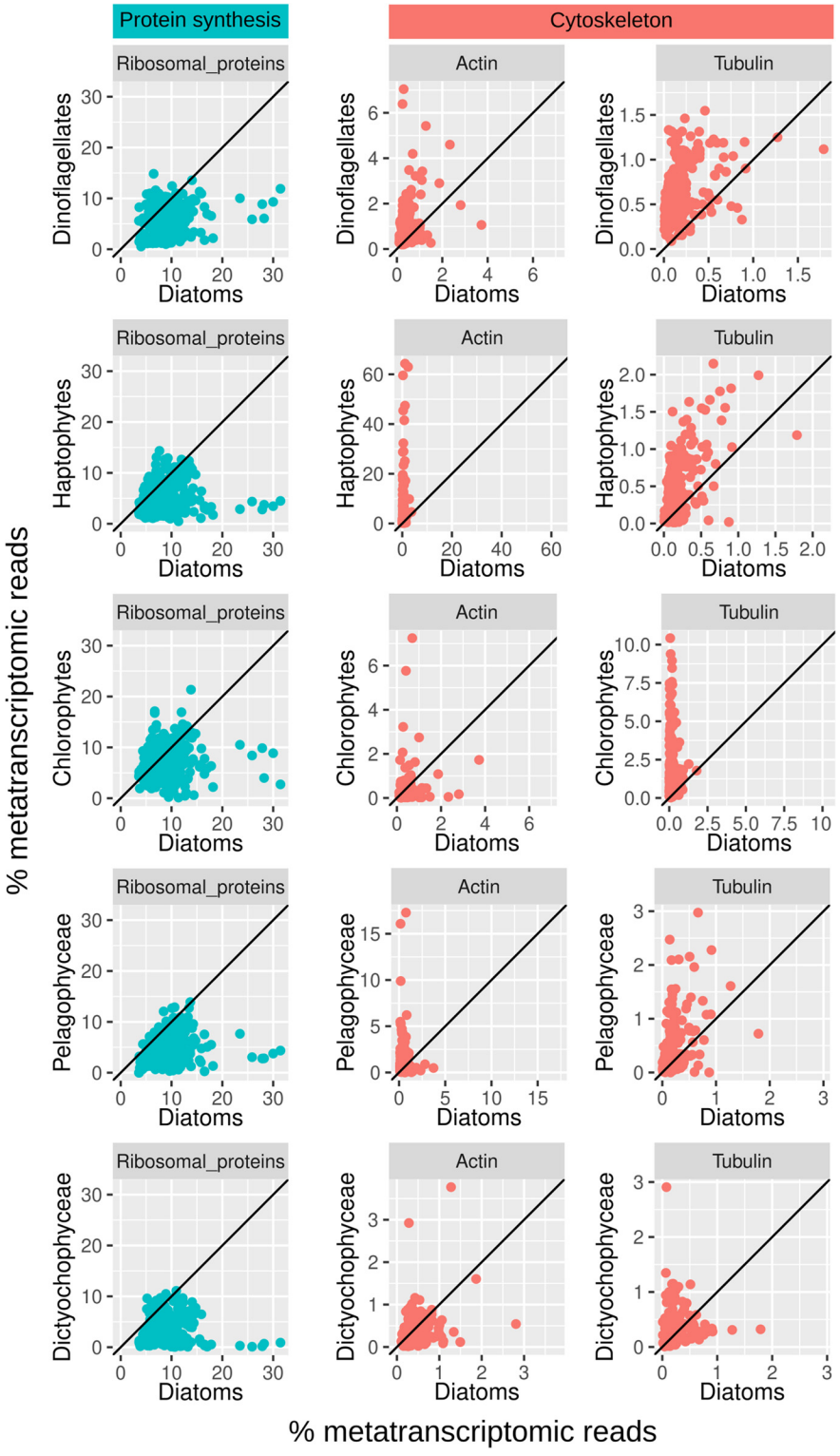

FIG 6 Transcriptional efforts to maintain proteins involved in protein synthesis (ribosomal proteins) and the cytoskeleton (actin and tubulin) in marine environmental populations of diatoms versus other photosynthetic protists. The analyzed data correspond to the metatranscriptomes generated by *Tara* Oceans across the main ocean regions (see Fig. S1 in the supplemental material) (52, 53). The scatterplots compare the relative abundances (proportion of metatranscriptomic reads for the given function among the total metatranscriptomic reads from the corresponding taxon) between diatoms and other photosynthetic protists. Each point corresponds to a size-fractionated seawater sample. Axes are on the same scale, and the diagonal lines correspond to a 1:1 slope.

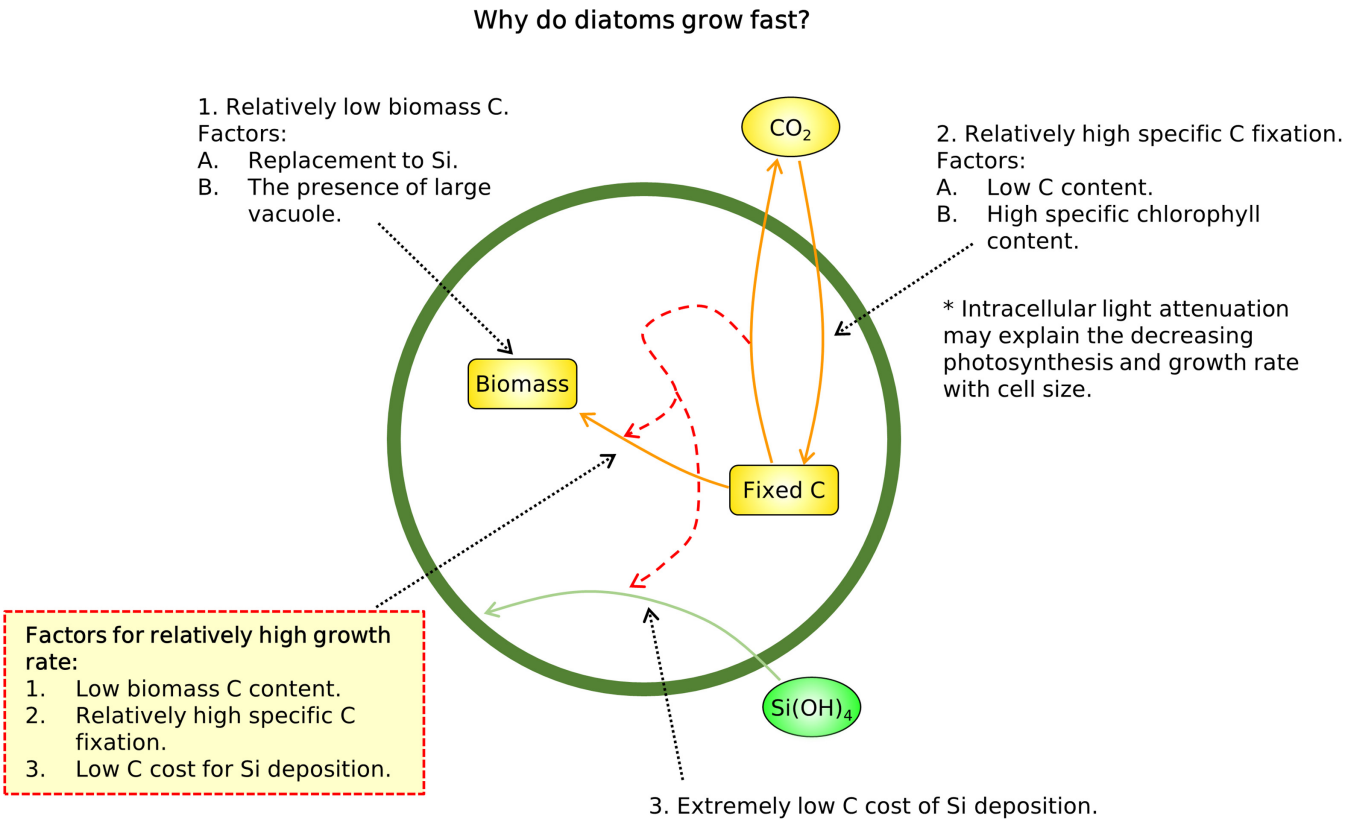

FIG 7 Schematic summary of this study. Key conclusions are within the dashed red frame.

this, our results highlight two factors that could generate variation in diatom growth rates even within a given size class. First, diatoms exhibit high variability in Q_C at each size, and this would translate directly into growth rate differences. Second, the degree of silicification can vary among species and according to other growth conditions. Further studies are needed to identify and incorporate additional factors into the model to improve its performance. One of these factors is likely to be iron, which is known to impact diatom growth strongly, as well as to influence frustule thickness (55–57). Additional uncertainty may involve the production of extracellular polysaccharides (58), which may reduce the overall growth rate because it contributes to the loss of C (see Fig. S3). However, such C excretion is not exclusive to diatoms (59–62), and how it affects the relative growth rate has not been clear. For example, if diatoms have lower C excretion than other phytoplankton, this may contribute to a higher growth rate of diatoms, but such a trend has not been well supported so far.

Conclusions. To investigate what causes high growth rates of diatoms under nutrient repletion, we have developed a simple metabolic model of diatoms (CFM-Diatom), focusing on C metabolism. The model captures the observed high maximum growth rates of diatoms relative to other phytoplankton, based on relatively low requirements for C for cellular material, resulting in high specific C fixation rates and an extremely low energetic cost for Si deposition (Fig. 7). These results led us to hypothesize that structural material, which is rich in C, is replaced by silica frustules, reducing cellular C requirements for growth and enriching growth-related molecules, such as those for light harvesting and C fixation, as well as for various molecular machineries (Fig. 7). This hypothesis is consistent with an interpretation of *Tara* Oceans data, which show that the transcript abundance for cytoskeleton components in diatoms is lower than in other phytoplankton, suggesting that the rigid support of the silica frustule can reduce the energy costs for maintaining their structure; the diatoms can then channel resources into growth, as reflected by the greater transcript abundance for ribosomal proteins. Our simple model focusing on metabolism may be useful for

investigating growth rate-volume relationships for other specific types of phytoplankton, such as calcifiers, diazotrophs, and cyanobacteria. CFM-Diatom may provide a mechanistic framework to predict the growth differences in ecosystem models, instead of relying on simple parameterizations. Finally, our study indicates the effective use of Si as a cellular structure instead of C, enabling diatoms to be the most productive primary producers in the global ocean.

MATERIALS AND METHODS

To study why diatoms may grow quickly and why their growth decreases with increased volume, we have developed CFM-Diatom (Fig. 3). The model represents simple coarse-grained fluxes based on mass, energy, and electron budgets and is useful for providing quantitative information on a cellular scale (33–35, 63, 64). The model's flexibility, computational efficiency, transparency, and ability to provide an intuitive whole-cell view complements more detailed models such as flux balance analysis (65–68). Here, to represent nutrient-replete situations (69), we focus on C fluxes in the model and test the effect of reduced C requirements in diatoms. We also simulate intracellular light attenuation and test the effect of volume on the growth rate. Furthermore, we explicitly represent silica deposition and quantify its C costs at a cellular scale. Finally, the importance of C savings by silica frustules is tested with *in situ* molecular data from environmental phytoplankton populations observed by the *Tara* Oceans expedition.

CFM-Diatom. Here, we describe the core equations of CFM-Diatom (Fig. 3). The parameter units and values are listed in Table S1 and S2 in the supplemental material. Since our focus is the maximum growth rate, we assume nutrient-saturated conditions (i.e., nitrogen, phosphorus, silicon, and iron are not limited). Under such conditions, the growth would be controlled by the rate of photosynthesis (or C fixation) (35, 69) and temperature (70, 71); here, we focus on the former and thus the C balance within the cell:

$$\frac{dQ_C}{dt} = F_{Pho} - \mu Q_C(1+E_\mu+E_{Si}) \tag{1}$$

where Q_C is the cellular C quota, t is time, F_{Pho} is the photosynthesis rate per cell, μ is the growth rate, E_μ is the growth respiration factor, and E_{Si} is a factor for silica deposition cost (24, 25). Assuming a steady state, we obtain a simple relation for growth rate:

$$\mu = \frac{F_{Pho}}{Q_C(1+E_\mu+E_{Si})} \tag{2}$$

Here, Q_C is calculated from a cell volume:

$$Q_C = A_C V^{B_C} \tag{3}$$

where A_C and B_C are constant factors (26) and V is cellular volume. We differentiate diatom cells and other phytoplankton cells with two factors. First, E_{Si} applies only to diatom cells, because the creation of silica frustules is specific to diatom cells. Second, we applied different A_C and B_C values for diatoms and other cells (see the supplemental material), since diatoms show a distinct Q_C-V pattern, with lower Q_C values than other phytoplankton (26). To obtain F_{Pho}, we considered the effect of light attenuation within the cell following Beer's Law (72) and a saturating curve of photosynthesis with light (see the supplemental material), which yields a decreased specific photosynthesis rate with size (Fig. 4A). Given the broad quantitative success of the simple model (Fig. 2), we hypothesize that the size-dependent light absorption coefficients have next-order impacts on the growth rate. Further experiments are needed to constrain such factors.

Analysis of *Tara* Oceans metatranscriptomes. *Tara* Oceans expeditions performed a worldwide sampling of plankton in the upper layers of the ocean between 2009 and 2013, covering the main ocean basins. A low-shear, nonintrusive, peristaltic pump and plankton nets of various mesh sizes were used on board *Tara* to sample and concentrate appropriate volumes of seawater to assess local eukaryotic biodiversity in four major organism size fractions, i.e., piconanoplankton (0.8 to 5 μm or 0.8 to 2,000 μm), nanoplankton (5 to 20 μm or 3 to 20 μm), microplankton (20 to 180 μm), and mesoplankton (180 to 2,000 μm) (see Fig. S1 of reference 53). Metatranscriptomes were generated from poly(A)$^+$ RNA extracted from these samples (52, 53). The metatranscriptomic reads were assembled and then clustered at 95% identity. We searched this catalog for sequences coding for ribosomal proteins (112 Pfam models listed in Table S1 of reference 38) and for the cytoskeleton components actin (Pfam entry code PF00022) and tubulin (Pfam entry code PF00091) by running HMMer (version 3.2.1 with the gathering threshold option) over the translated sequences. Taxonomic assignment was carried out by sequence similarity against a reference database (52). Based on this assignment, we retained only sequences assigned to the main phytoplankton groups (note that we were not able to discard heterotrophic species from dinoflagellates due to the small number of reference sequences for this group). We finally retrieved the metatranscriptomic read abundances of the selected sequences and normalized them to the total read abundance for transcripts of the corresponding phytoplankton taxon in each sample. The resulting relative abundance values were compared between diatoms and other photosynthetic protists to infer the differences in the transcriptional efforts to maintain protein

synthesis and the cytoskeleton. We focused the analysis on the surface samples (5-m depth) from the 66 stations (see Fig. S1) for which metatranscriptomic data are available.

Data availability. CFM-Diatom is written in Python 3.2.5 and is freely available from Zenodo (https://doi.org/10.5281/zenodo.3750213).

SUPPLEMENTAL MATERIAL

Supplemental material is available online only.

SUPPLEMENTAL FILE 1, PDF file, 0.9 MB.

ACKNOWLEDGMENTS

We thank Michael J. Follows and Susumu Yoshizawa for useful discussions. This work was supported by grants from the Japan Student Service Organization (L11171020001 to K.I.), the Simons Foundation (544338 to K.I. and 549931FY22 to S.D.), and the Gordon and Betty Moore Foundation (GBMF 3775 to C.D.). J.J.P.K. and C.B. additionally acknowledge European Research Council Advanced Awards Diatomite and Diatomic under the European Union Horizon 2020 research and innovation program (grant agreements 294823 and 835067), the Fonds Français pour l'Environnement Mondial, the French government Investissements d'Avenir Programmes MEMO LIFE (grant ANR-10-LABX-54), the Université de Recherche Paris Sciences et Lettres (grant ANR-1253-11-IDEX-0001-02), and OCEANOMICS (grant ANR-11-BTBR-0008). We are grateful for the support.

REFERENCES

1. Mann DG. 1999. The species concept in diatoms. Phycologia 38:437–495. https://doi.org/10.2216/i0031-8884-38-6-437.1.
2. Hecky RE, Mopper K, Kilham P, Degens ET. 1973. The amino acid and sugar composition of diatom cell-walls. Mar Biol 19:323–331. https://doi.org/10.1007/BF00348902.
3. Reimann BEF, Leivin JC, Volcani BE. 1966. Studies on the biochemistry and fine structure of silica shell formation in diatoms. II. The structure of the cell wall of *Navicula pelliculosa* (Bréb.) Hilse. J Phycol 2:74–84. https://doi.org/10.1111/j.1529-8817.1966.tb04597.x.
4. Sumper M, Brunner E. 2006. Learning from diatoms: nature's tools for the production of nanostructured silica. Adv Funct Mater 16:17–26. https://doi.org/10.1002/adfm.200500616.
5. Popovich CA, Gayoso AM. 1999. Effect of irradiance and temperature on the growth rate of *Thalassiosira curviseriata* Takano (Bacillariophyceae), a bloom diatom in Bahia Blanca estuary (Argentina). J Plankton Res 21:1101–1110. https://doi.org/10.1093/plankt/21.6.1101.
6. Hildebrand M, Lerch SJL, Shrestha RP. 2018. Understanding diatom cell wall silicification-moving forward. Front Mar Sci https://doi.org/10.3389/fmars.2018.00125.
7. Behrenfeld MJ, Halsey KH, Boss E, Karp-Boss L, Milligan AJ, Peers G. 2021. Thoughts on the evolution and ecological niche of diatoms. Ecol Monogr 91: e01457. https://doi.org/10.1002/ecm.1457.
8. Durkin CA, Marchetti A, Bender SJ, Truong T, Morales R, Mock T, Armbrust EV. 2012. Frustule-related gene transcription and the influence of diatom community composition on silica precipitation in an iron-limited environment. Limnol Oceanogr 57:1619–1633. https://doi.org/10.4319/lo.2012.57.6.1619.
9. Alexander H, Rouco M, Haley ST, Wilson ST, Karl DM, Dyhrman ST. 2015. Functional group-specific traits drive phytoplankton dynamics in the oligotrophic ocean. Proc Natl Acad Sci U S A 112:E5972–E5979. https://doi.org/10.1073/pnas.1518165112.
10. Lampe RH, Cohen NR, Ellis KA, Bruland KW, Maldonado MT, Peterson TD, Till CP, Brzezinski MA, Bargu S, Thamatrakoln K, Kuzminov FI, Twining BS, Marchetti A. 2018. Divergent gene expression among phytoplankton taxa in response to upwelling. Environ Microbiol 20:3069–3082. https://doi.org/10.1111/1462-2920.14361.
11. Burckle LH. 1984. Diatom distribution and paleoceanographic reconstruction in the Southern Ocean: present and last glacial maximum. Mar Micropaleontol 9:241–261. https://doi.org/10.1016/0377-8398(84)90015-X.
12. Hirata T, Hardman-Mountford NJ, Brewin RJW, Aiken J, Barlow R, Suzuki K, Isada T, Howell E, Hashioka T, Noguchi-Aita M, Yamanaka Y. 2011. Synoptic relationships between surface chlorophyll-*a* and diagnostic pigments specific to phytoplankton functional types. Biogeosciences 8:311–327. https://doi.org/10.5194/bg-8-311-2011.
13. Malviya S, Scalco E, Audic S, Vincent F, Veluchamy A, Poulain J, Wincker P, Iudicone D, de Vargas C, Bittner L, Zingone A, Bowler C. 2016. Insights into global diatom distribution and diversity in the world's ocean. Proc Natl Acad Sci U S A 113:E1516–E1525. https://doi.org/10.1073/pnas.1509523113.
14. Chai F, Dugdale RC, Peng T-H, Wilkerson FPB. 2002. One-dimensional ecosystem model of the equatorial Pacific upwelling system. Part II: sensitivity analysis and comparison with JGOFS EqPac data. Deep Sea Res 2 Top Stud Oceanogr 49:2747–2768. https://doi.org/10.1016/S0967-0645(02)00056-5.
15. Irwin AJ, Finkel ZV, Schofield OME, Falkowski PG. 2006. Scaling-up from nutrient physiology to the size-structure of phytoplankton communities. J Plankton Res 28:459–471. https://doi.org/10.1093/plankt/fbi148.
16. Follett CL, Dutkiewicz S, Karl DM, Inomura K, Follows MJ. 2018. Seasonal resource conditions favor a summertime increase in North Pacific diatom–diazotroph associations. ISME J 12:1543–1557. https://doi.org/10.1038/s41396-017-0012-x.
17. Gregg WW, Casey NW. 2007. Modeling coccolithophores in the global oceans. Deep Sea Res 2 Top Stud Oceanogr 54:447–477. https://doi.org/10.1016/j.dsr2.2006.12.007.
18. Dutkiewicz S, Hickman AE, Jahn O, Gregg WW, Mouw CB, Follows MJ. 2015. Capturing optically important constituents and properties in a marine biogeochemical and ecosystem model. Biogeosciences 12:4447–4481. https://doi.org/10.5194/bg-12-4447-2015.
19. Dutkiewicz S, Cermeno P, Jahn O, Follows MJ, Hickman AE, Taniguchi DAA, Ward BA. 2020. Dimensions of marine phytoplankton diversity. Biogeosciences 17:609–634. https://doi.org/10.5194/bg-17-609-2020.
20. Le Quéré C, Harrison SP, Prentice IC, Buitenhuis ET, Aumont O, Bopp L. 2005. Ecosystem dynamics based on plankton functional types for global ocean biogeochemistry models. Glob Chang Biol 11:2016–2040. https://doi.org/10.1111/j.1365-2486.2005.1004.x.
21. Kremer CT, Thomas MK, Litchman E. 2017. Temperature- and size-scaling of phytoplankton population growth rates: reconciling the Eppley curve and the metabolic theory of ecology. Limnol Oceanogr 62:1658–1670. https://doi.org/10.1002/lno.10523.
22. Anderson SI, Barton AD, Clayton S, Dutkiewicz S, Rynearson TA. 2021. Marine phytoplankton functional types exhibit diverse responses to thermal change. Nat Commun 12:6413. https://doi.org/10.1038/s41467-021-26651-8.
23. Taniguchi DAA, Franks PJS, Poulin FJ. 2014. Planktonic biomass size spectra: an emergent property of size-dependent physiological rates, food web dynamics, and nutrient regimes. Mar Ecol Prog Ser 514:13–33. https://doi.org/10.3354/meps10968.
24. Werner D. 1977. Silicate metabolism, p 110–149. *In* Werner D (ed), The biology of the diatoms. University of California Press, Berkeley, CA.
25. Raven J. 1983. The transport and function of silicon in plants. Biol Rev 58:179–207. https://doi.org/10.1111/j.1469-185X.1983.tb00385.x.
26. Menden-Deuer S, Lessard EJ. 2000. Carbon to volume relationships for dinoflagellates, diatoms, and other protist plankton. Limnol Oceanogr 45:569–579. https://doi.org/10.4319/lo.2000.45.3.0569.

27. Tang EPY. 1995. The allometry of algal growth rates. J Plankton Res 17:1325–1335. https://doi.org/10.1093/plankt/17.6.1325.
28. Marañón E, Cermeño P, López-Sandoval DC, Rodríguez-Ramos T, Sobrino C, Huete-Ortega M, Blanco JM, Rodríguez J. 2013. Unimodal size scaling of phytoplankton growth and the size dependence of nutrient uptake and use. Ecol Lett 16:371–379. https://doi.org/10.1111/ele.12052.
29. López-Sandoval DC, Rodríguez-Ramos T, Cermeño P, Sobrino C, Marañón E. 2014. Photosynthesis and respiration in marine phytoplankton: relationship with cell size, taxonomic affiliation, and growth phase. J Exp Mar Biol Ecol 457:151–159. https://doi.org/10.1016/j.jembe.2014.04.013.
30. Marañón E. 2015. Cell size as a key determinant of phytoplankton metabolism and community structure. Annu Rev Mar Sci 7:241–264. https://doi.org/10.1146/annurev-marine-010814-015955.
31. Wirtz KW. 2011. Non-uniform scaling in phytoplankton growth rate due to intracellular light and CO_2 decline. J Plankton Res 33:1325–1341. https://doi.org/10.1093/plankt/fbr021.
32. Finkel ZV. 2001. Light absorption and size scaling of light-limited metabolism in marine diatoms. Limnol Oceanogr 46:86–94. https://doi.org/10.4319/lo.2001.46.1.0086.
33. Inomura K, Bragg J, Follows MJ. 2017. A quantitative analysis of the direct and indirect costs of nitrogen fixation: a model based on *Azotobacter vinelandii*. ISME J 11:166–175. https://doi.org/10.1038/ismej.2016.97.
34. Inomura K, Masuda T, Gauglitz JM. 2019. Active nitrogen fixation by *Crocosphaera* expands their niche despite the presence of ammonium: a case study. Sci Rep 9:15064. https://doi.org/10.1038/s41598-019-51378-4.
35. Inomura K, Follett CL, Masuda T, Eichner M, Prášil O, Deutsch C. 2020. Carbon transfer from the host diatom enables fast growth and high rate of N_2 fixation by symbiotic heterocystous cyanobacteria. Plants 9:192. https://doi.org/10.3390/plants9020192.
36. Chan AT. 1978. Comparative physiological study of marine diatoms and dinoflagellates in relation to irradiance and cell size. I. Growth under continuous light. J Phycol 14:396–402. https://doi.org/10.1111/j.1529-8817.1978.tb02458.x.
37. Matsuda Y, Hopkinson BM, Nakajima K, Dupont CL, Tsuji Y. 2017. Mechanisms of carbon dioxide acquisition and CO_2 sensing in marine diatoms: a gateway to carbon metabolism. Philos Trans R Soc B 372:20160403. https://doi.org/10.1098/rstb.2016.0403.
38. Pierella Karlusich JJ, Bowler C, Biswas H. 2021. Carbon dioxide concentration mechanisms in natural populations of marine diatoms: insights from *Tara* Oceans. Front Plant Sci 12:657821. https://doi.org/10.3389/fpls.2021.657821.
39. Kikutani S, Nakajima K, Nagasato C, Tsuji Y, Miyatake A, Matsuda Y. 2016. Thylakoid luminal θ-carbonic anhydrase critical for growth and photosynthesis in the marine diatom *Phaeodactylum tricornutum*. Proc Natl Acad Sci U S A 113:9828–9833. https://doi.org/10.1073/pnas.1603112113.
40. Bailleul B, Berne N, Murik O, Petroutsos D, Prihoda J, Tanaka A, Villanova V, Bligny R, Flori S, Falconet D, Krieger-Liszkay A, Santabarbara S, Rappaport F, Joliot P, Tirichine L, Falkowski PG, Cardol P, Bowler C, Finazzi G. 2015. Energetic coupling between plastids and mitochondria drives CO_2 assimilation in diatoms. Nature 524:366–369. https://doi.org/10.1038/nature14599.
41. Goessling JW, Yanyan S, Kühl M, Ellegaard M. 2021. Frustule photonics and light harvesting strategies in diatoms, p 269–300. *In* Annenkov V, Seckback J, Gordon R (ed), Diatom morphogenesis. Wiley, Hoboken, NJ.
42. Claquin P, Martin-Jézéquel V, Kromkamp JC, Veldhuis MJW, Kraay GW. 2002. Uncoupling of silicon compared with carbon and nitrogen metabolisms and the role of the cell cycle in continuous cultures of *Thalassiosira pseudonana* (Bacillariophyceae) under light, nitrogen, and phosphorus control. J Phycol 38:922–930. https://doi.org/10.1046/j.1529-8817.2002.t01-1-01220.x.
43. Martin-Jézéquel V, Hildebrand M, Brzezinski MA. 2000. Silicon metabolism in diatoms: implications for growth. J Phycol 36:821–840. https://doi.org/10.1046/j.1529-8817.2000.00019.x.
44. Hoffmann LJ, Peeken I, Lochte K. 2008. Iron, silicate, and light co-limitation of three Southern Ocean diatom species. Polar Biol 31:1067–1080. https://doi.org/10.1007/s00300-008-0448-6.
45. Wang S, Arellano-Santoyo H, Combs PA, Shaevitz JW. 2010. Actin-like cytoskeleton filaments contribute to cell mechanics in bacteria. Proc Natl Acad Sci U S A 107:9182–9185. https://doi.org/10.1073/pnas.0911517107.
46. Taylor MP, Koyuncu OO, Enquist LW. 2011. Subversion of the actin cytoskeleton during viral infection. Nat Rev Microbiol 9:427–439. https://doi.org/10.1038/nrmicro2574.
47. Geider RJ, Moore CM, Ross ON. 2009. The role of cost-benefit analysis in models of phytoplankton growth and acclimation. Plant Ecol Divers 2:165–178. https://doi.org/10.1080/17550870903300949.
48. Lürling M, Van Donk E. 1997. Life history consequences for *Daphnia pulex* feeding on nutrient-limited phytoplankton. Freshw Biol 38:693–709. https://doi.org/10.1046/j.1365-2427.1997.00242.x.
49. Hessen DO, De Lange HJ, Van Donk E. 1997. UV-induced changes in phytoplankton cells and its effects on grazers. Freshw Biol 38:513–524. https://doi.org/10.1046/j.1365-2427.1997.00223.x.
50. Boehlke KW, Friesen JD. 1975. Cellular content of ribonucleic acid and protein in *Saccharomyces cerevisiae* as a function of exponential growth rate: calculation of the apparent peptide chain elongation rate. J Bacteriol 121:429–433. https://doi.org/10.1128/jb.121.2.429-433.1975.
51. Scott M, Gunderson CW, Mateescu EM, Zhang Z, Hwa T. 2010. Interdependence of cell growth and gene expression: origins and consequences. Science 330:1099–1102. https://doi.org/10.1126/science.1192588.
52. Carradec Q, Pelletier E, Da Silva C, Alberti A, Seeleuthner Y, Blanc-Mathieu R, Lima-Mendez G, Rocha F, Tirichine L, Labadie K, Kirilovsky A, Bertrand A, Engelen S, Madoui M-A, Méheust R, Poulain J, Romac S, Richter DJ, Yoshikawa G, Dimier C, Kandels-Lewis S, Picheral M, Searson S, Tara Oceans Coordinators, Jaillon O, Aury J-M, Karsenti E, Sullivan MB, Sunagawa S, Bork P, Not F, Hingamp P, Raes J, Guidi L, Ogata H, de Vargas C, Iudicone D, Bowler C, Wincker P. 2018. A global ocean atlas of eukaryotic genes. Nat Commun 9:373. https://doi.org/10.1038/s41467-017-02342-1.
53. Zayed AA, Wainaina JM, Dominguez-Huerta G, Pelletier E, Guo J, Mohssen M, Tian F, Pratama AA, Bolduc B, Zablocki O, Cronin D, Solden L, Delage E, Alberti A, Aury J-M, Carradec Q, da Silva C, Labadie K, Poulain J, Ruscheweyh H-J, Salazar G, Shatoff E, Tara Oceans Coordinators, Bundschuh R, Fredrick K, Kubatko LS, Chaffron S, Culley AI, Sunagawa S, Kuhn JH, Wincker P, Sullivan MB, Acinas SG, Babin M, Bork P, Boss E, Bowler C, Cochrane G, de Vargas C, Gorsky G, Guidi L, Grimsley N, Hingamp P, Iudicone D, Jaillon O, Kandels S, Karp-Boss L, Karsenti E, Not F, Ogata H, Poulton N, Pesant S, Sardet C, Speich S, Stemmann L, Sullivan MB, Sungawa S, Wincker P. 2022. Cryptic and abundant marine viruses at the evolutionary origins of Earth's RNA virome. Science 376:156–162. https://doi.org/10.1126/science.abm5847.
54. Tréguer P, Bowler C, Moriceau B, Dutkiewicz S, Gehlen M, Aumont O, Bittner L, Dugdale R, Finkel Z, Iudicone D, Jahn O, Guidi L, Lasbleiz M, Leblanc K, Levy M, Pondaven P. 2018. Influence of diatom diversity on the ocean biological carbon pump. Nat Geosci 11:27–37. https://doi.org/10.1038/s41561-017-0028-x.
55. Allen AE, LaRoche J, Maheswari U, Lommer M, Schauer N, Lopez PJ, Finazzi G, Fernie AR, Bowler C. 2008. Whole-cell response of the pennate diatom *Phaeodactylum tricornutum* to iron starvation. Proc Natl Acad Sci U S A 105:10438–10443. https://doi.org/10.1073/pnas.0711370105.
56. Hutchins DA, Bruland KW. 1998. Iron-limited growth and Si:N ratios in a coastal upwelling regime. Nature 393:561–564. https://doi.org/10.1038/31203.
57. Marchetti A, Cassar N. 2009. Diatom elemental and morphological changes in response to iron limitation: a brief review with potential paleoceanographic applications. Geobiology 7:419–431. https://doi.org/10.1111/j.1472-4669.2009.00207.x.
58. Shniukova EI, Zolotareva EK. 2015. Diatom exopolysaccharides: a review. Int J Algae 17:50–67. https://doi.org/10.1615/InterJAlgae.v17.i1.50.
59. Zhang S, Jiang Y, Chen C-S, Spurgin J, Schwehr KA, Quigg A, Chin W-C, Santschi PH. 2012. Aggregation, dissolution, and stability of quantum dots in marine environments: importance of extracellular polymeric substances. Environ Sci Technol 46:8764–8772. https://doi.org/10.1021/es301000m.
60. Decho AW, Gutierrez T. 2017. Microbial extracellular polymeric substances (EPSs) in ocean systems. Front Microbiol 8:922. https://doi.org/10.3389/fmicb.2017.00922.
61. Passow U. 2000. Formation of transparent exopolymer particles, TEP, from dissolved precursor material. Mar Ecol Prog Ser 192:1–11. https://doi.org/10.3354/meps192001.
62. Santschi PH, Xu C, Schwehr KA, Lin P, Sun L, Chin W-C, Kamalanathan M, Bacosa HP, Quigg A. 2020. Can the protein/carbohydrate (P/C) ratio of exopolymeric substances (EPS) be used as a proxy for their 'stickiness' and aggregation propensity? Mar Chem 218:103734. https://doi.org/10.1016/j.marchem.2019.103734.
63. Inomura K, Bragg J, Riemann L, Follows MJ. 2018. A quantitative model of nitrogen fixation in the presence of ammonium. PLoS One 13:e0208282. https://doi.org/10.1371/journal.pone.0208282.
64. Inomura K, Deutsch C, Wilson ST, Masuda T, Lawrenz E, Bučinská L, Sobotka R, Gauglitz JM, Saito MA, Prášil O, Follows MJ. 2019. Quantifying oxygen management and temperature and light dependencies of nitrogen fixation by *Crocosphaera watsonii*. mSphere 4:e00531-19. https://doi.org/10.1128/mSphere.00531-19.
65. Orth JD, Thiele I, Palsson BØ. 2010. What is flux balance analysis? Nat Biotechnol 28:245–248. https://doi.org/10.1038/nbt.1614.

66. Levitan O, Dinamarca J, Zelzion E, Lun DS, Guerra LT, Kim MK, Kim J, Van Mooy BAS, Bhattacharya D, Falkowski PG. 2015. Remodeling of intermediate metabolism in the diatom *Phaeodactylum tricornutum* under nitrogen stress. Proc Natl Acad Sci U S A 112:412–417. https://doi.org/10.1073/pnas.1419818112.
67. Singh D, Carlson R, Fell D, Poolman M. 2015. Modelling metabolism of the diatom *Phaeodactylum tricornutum*. Biochem Soc Trans 43:1182–1186. https://doi.org/10.1042/BST20150152.
68. Kim J, Fabris M, Baart G, Kim MK, Goossens A, Vyverman W, Falkowski PG, Lun DS. 2016. Flux balance analysis of primary metabolism in the diatom *Phaeodactylum tricornutum*. Plant J 85:161–176. https://doi.org/10.1111/tpj.13081.
69. Inomura K, Wilson ST, Deutsch C. 2019. Mechanistic model for the coexistence of nitrogen fixation and photosynthesis in marine *Trichodesmium*. mSystems 4:e00210-19. https://doi.org/10.1128/mSystems.00210-19.
70. Eppley R. 1972. Temperature and phytoplankton growth in the sea. Fishery Bull 70:1063–1085.
71. Montagnes DJS, Franklin DJ. 2001. Effect of temperature on diatom volume, growth rate, and carbon and nitrogen content: reconsidering some paradigms. Limnol Oceanogr 46:2008–2018. https://doi.org/10.4319/lo.2001.46.8.2008.
72. Liou KN. 2002. An introduction to atmospheric radiation, 2nd ed. Academic Press, San Diego, CA.